nature research

https://doi.org/10.1038/s41560-020-00705-5

Supplementary information

All-perovskite tandem solar cells with 24.2% certified efficiency and area over 1 cm^2 using surface-anchoring zwitterionic antioxidant

In the format provided by the authors and unedited

Supplementary Information for

All-perovskite tandem solar cells with 24.2% certified efficiency and area over 1 cm^2 using surface-anchoring zwitterionic antioxidant

Ke Xiao[1,2†], Renxing Lin[1†], Qiaolei Han[1†], Yi Hou[3], Zhenyuan Qin[4], Hieu T. Nguyen[5], Jin Wen[1], Mingyang Wei[3], Vishal Yeddu[6], Makhsud I. Saidaminov[6], Yuan Gao[1], Xin Luo[1,2], Yurui Wang[1], Han Gao[1], Chunfeng Zhang[4], Jun Xu[2], Jia Zhu[1], Edward H. Sargent[3], and Hairen Tan[1]*

[1]National Laboratory of Solid State Microstructures, Collaborative Innovation Center of Advanced Microstructures, Jiangsu Key Laboratory of Artificial Functional Materials, College of Engineering and Applied Sciences, Nanjing University, Nanjing, China.

[2]School of Electronics Science and Engineering, Nanjing University, Nanjing, China.

[3]Department of Electrical and Computer Engineering, University of Toronto, Toronto, Ontario, Canada.

[4]School of Physics, Nanjing University, Nanjing, China.

[5]Research School of Electrical, Energy and Materials Engineering, College of Engineering and Computer Science, The Australian National University, Canberra, Australia.

[6]Department of Chemistry, University of Victoria, Victoria, BC, Canada.

[*]Correspondence to: hairentan@nju.edu.cn (H.T.)

[†]These authors contributed equally: K. Xiao, R. Lin, Q. Han

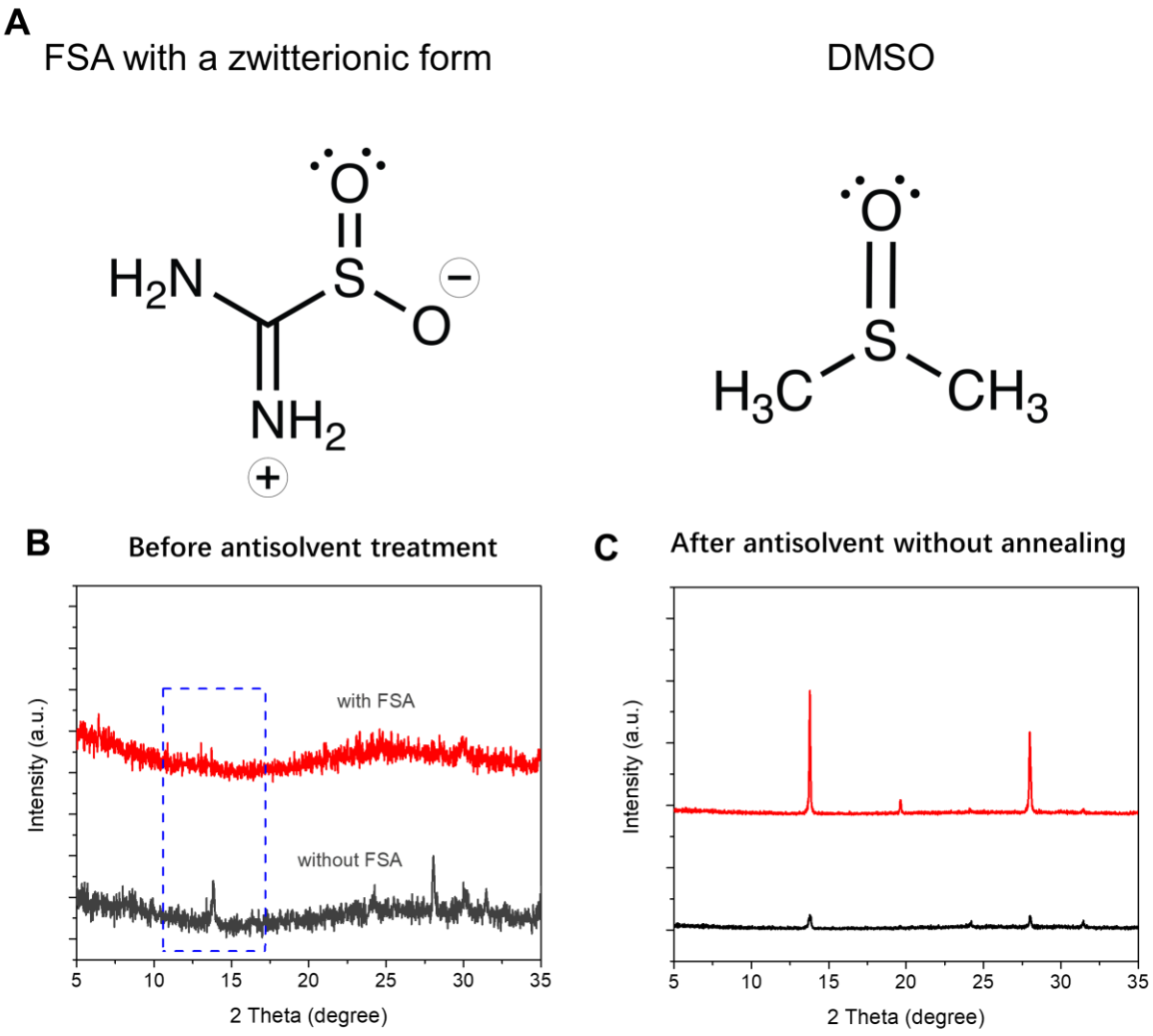

Supplementary Figure 1. Structure of formamidine sulfinic acid (FSA). (A) Chemical structures of FSA and DMSO molecules. The FSA is a strong reducing agent (antioxidant) and has a zwitterionic structure. Both FSA and DMSO molecules have an oxygen donor (with two lone-pair electrons) and are similar in term of acting as electron-donor to form adduct with Pb/Sn metal halides (acting as electron-acceptor). In addition, FSA can coordinate with metal halides via the sulfinic group. (B-C) XRD patterns of mixed Pb-Sn films processed from perovskite precursor solutions without and with FSA. (B) Before the antisolvent treatment; (C) after the antisolvent treatment but without thermal annealing.

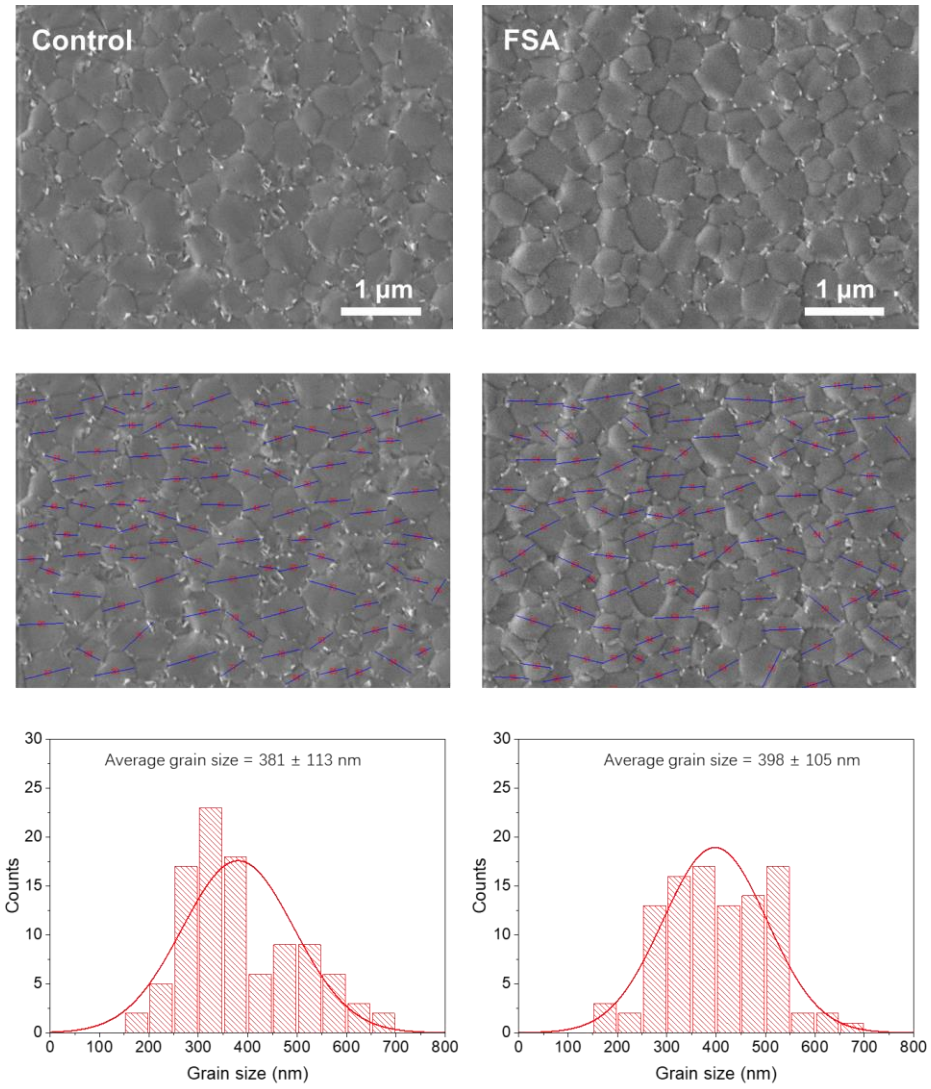

Supplementary Figure 2. SEM images and grain size analysis of control and FSA mixed Pb-Sn perovskite films. The two films exhibited similar morphology and grain size.

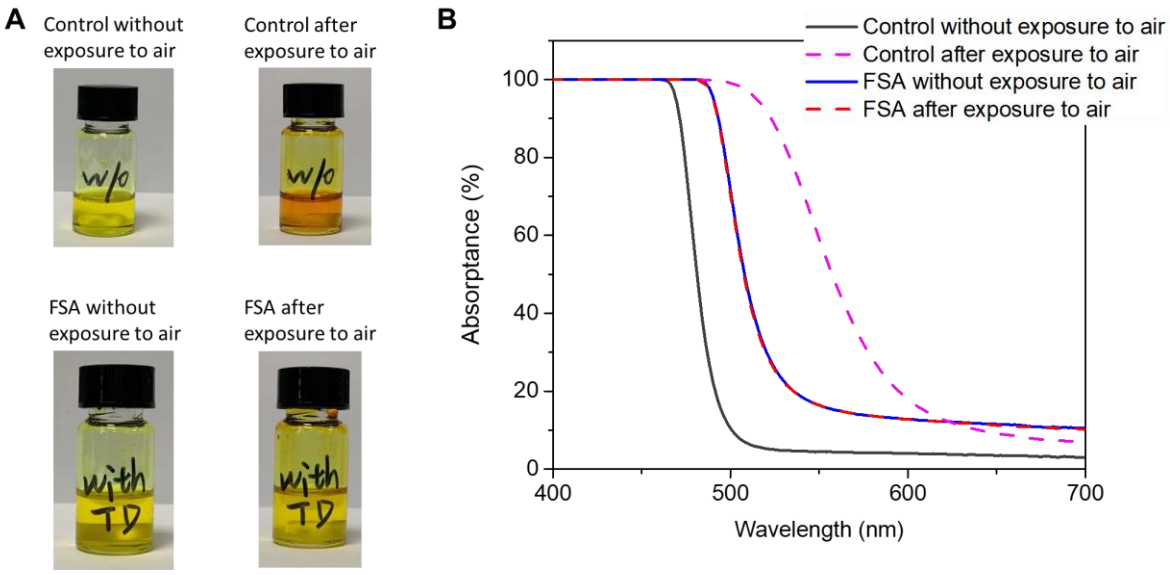

Supplementary Figure 3. Photographs (A) and absorption spectra (B) of control and FSA mixed Pb-Sn perovskite precursor solutions without and with exposure to ambient air. The control solution (without Sn powders, marked as w/o) exhibited obvious color change from yellow to red after exposure to air for a few minutes due to the oxidation of Sn^{2+} to Sn^{4+}, corresponding to the significant red shift of transmission spectra. The FSA solution (without Sn powders, marked as with TD) showed no observable change in color after a few minutes' exposure to air because of the strong reductivity of FSA. Correspondingly, there was no change in the absorption spectra before and after exposure to air. The color change and the corresponding shift in absorption onset of precursor solution (solution without air exposure) after adding FSA additive indicate the coordination between FSA and PbI_2/SnI_2.

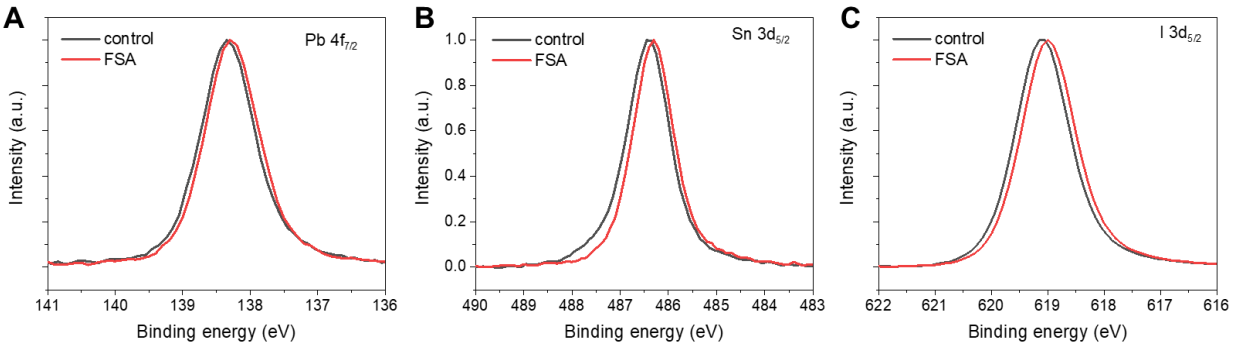

Supplementary Figure 4. XPS spectra of control and FSA mixed Pb-Sn perovskite films. (**A**) Pb $4f_{7/2}$; (**B**) Sn $3d_{5/2}$; and (**C**) I $3d_{5/2}$.

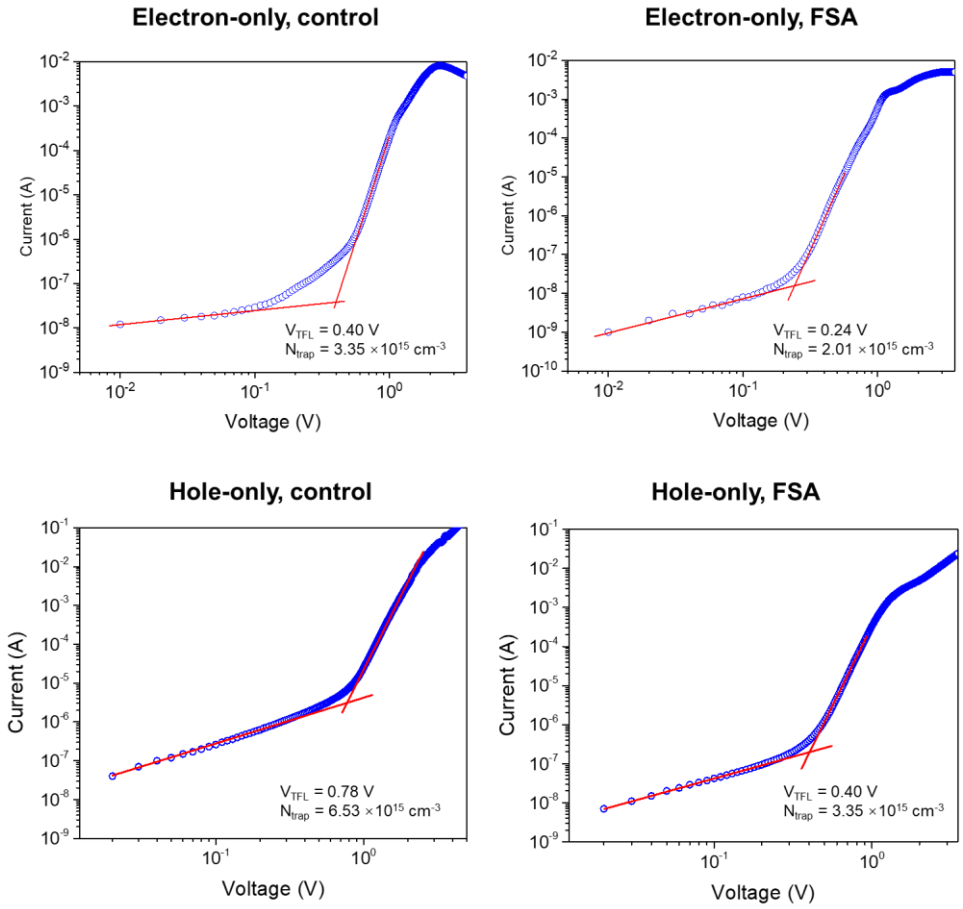

Supplementary Figure 5. Current-voltage traces and trap density of Pb-Sn narrow-bandgap perovskites as determined by the space-charge-limited current (SCLC) method. Electron-only and hole-only device structures were constructed to obtain the electron trap density and hole trap density, respectively. The trap density N_{trap} is determined by the equation: $V_{TFL}=qN_{trap}L^2/(2\varepsilon\varepsilon_0)$, where V_{TFL} is trap-filled limit voltage, L the thickness of perovskite film, ε the relative dielectric constant of perovskite, and ε_0 the vacuum permittivity.

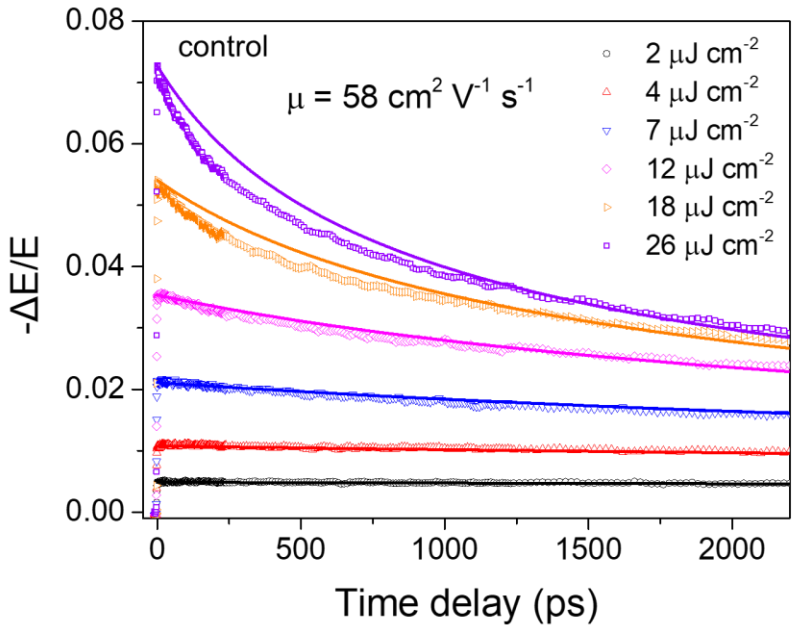

Supplementary Figure 6. Femtosecond OPTP transients of control mixed Pb-Sn perovskite film measured after excitation with a 90-fs light pulse of 800 nm wavelength with various fluences. The transients were fitted globally according to the equation $dn(t)/dt = -k_3n^3 - k_2n^2 - k_1n$, where t is decay time, and k_1, k_2, k_3 are rate constants associated with monomolecular recombination, bimolecular recombination and Auger recombination, respectively. The mobility is calculated to 58 $cm^2\ V^{-1}\ s^{-1}$. The diffusion lengths of control and FSA samples (Fig. 2c) at 1-sun condition are estimated to 3.1 and 5.6 μm using carrier lifetimes (64 and 188 ns) derived from the PL decays, respectively.

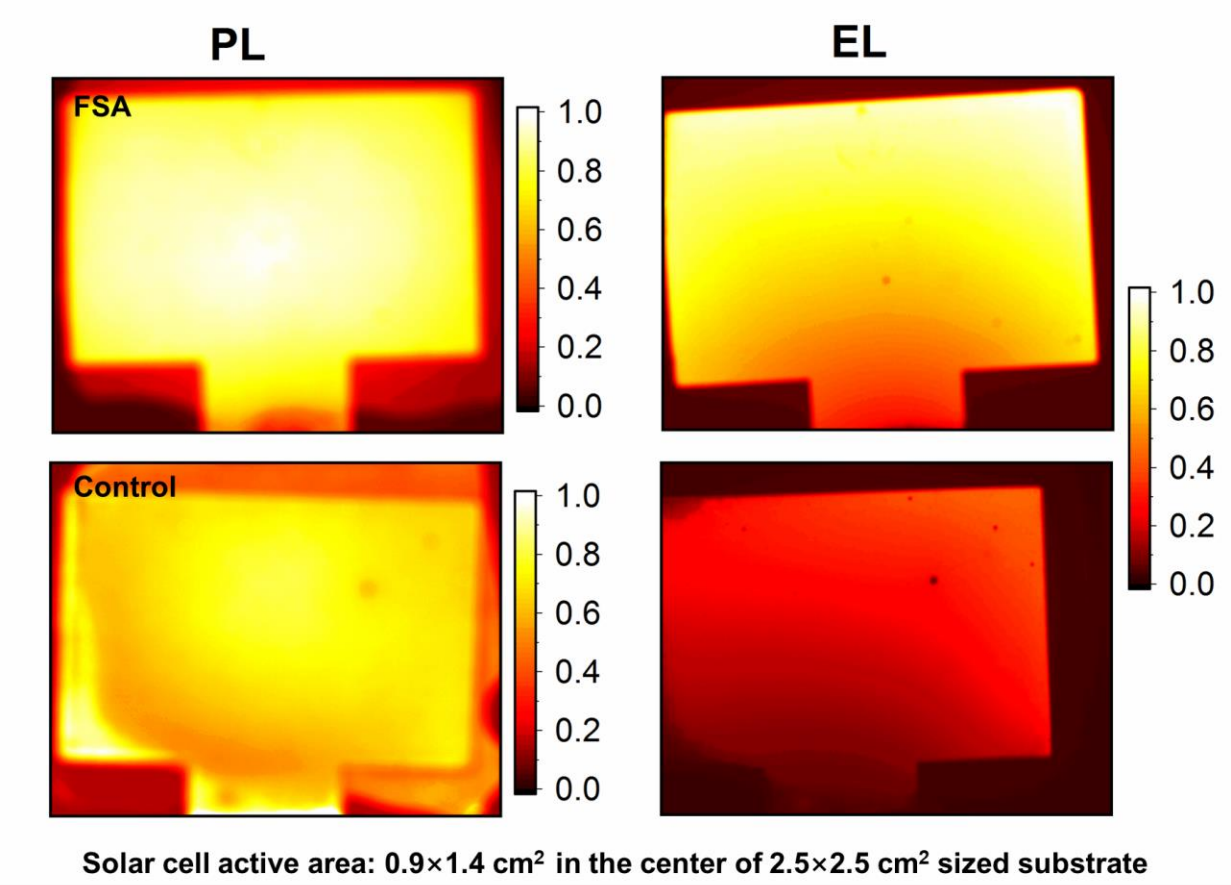

Supplementary Figure 7. PL and EL imaging of Pb-Sn perovskite solar cells. PL and EL intensity imaging over the active areas (0.9×1.4 cm^2) of the control and FSA mixed Pb-Sn perovskite solar cells (substrate size of 2.5×2.5 cm^2). The PL excitation and detection was from the front glass side.

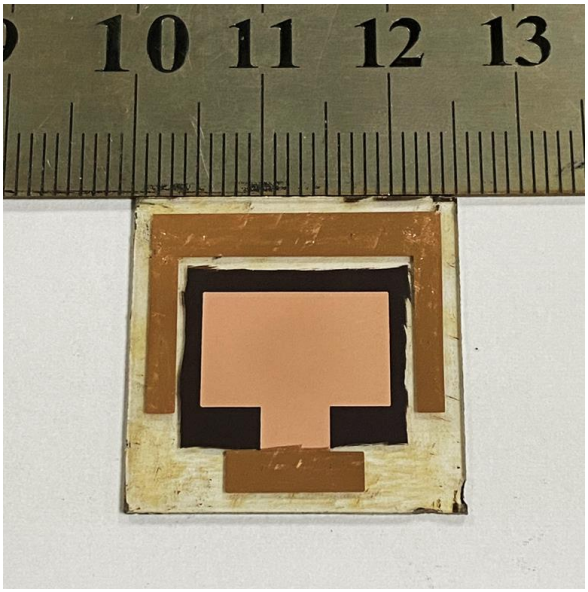

Supplementary Figure 8. Photograph of a Pb-Sn solar cell with an aperture area of 1.05 cm^2. The device was deposited on a 2.5×2.5 cm^2 substrate with an active area of 0.9×1.4 cm^2 at the center.

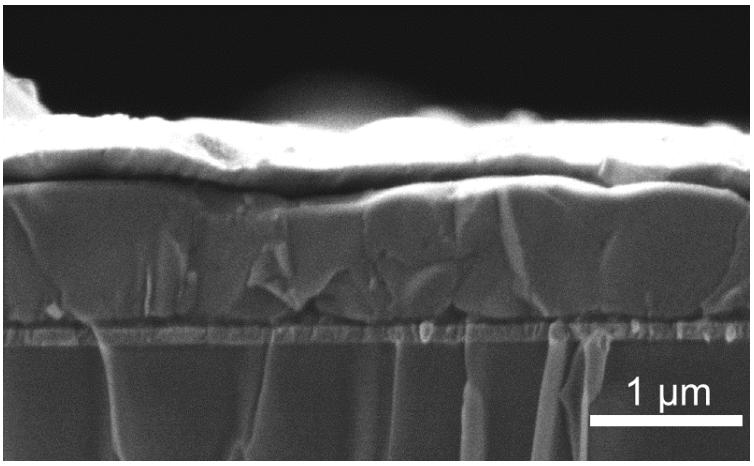

Supplementary Figure 9. Cross-sectional SEM image of a large-area FSA mixed Pb-Sn solar cell. The thickness of the Pb-Sn perovskite absorber layer is about 850 nm (precursor concentration 1.8 M).

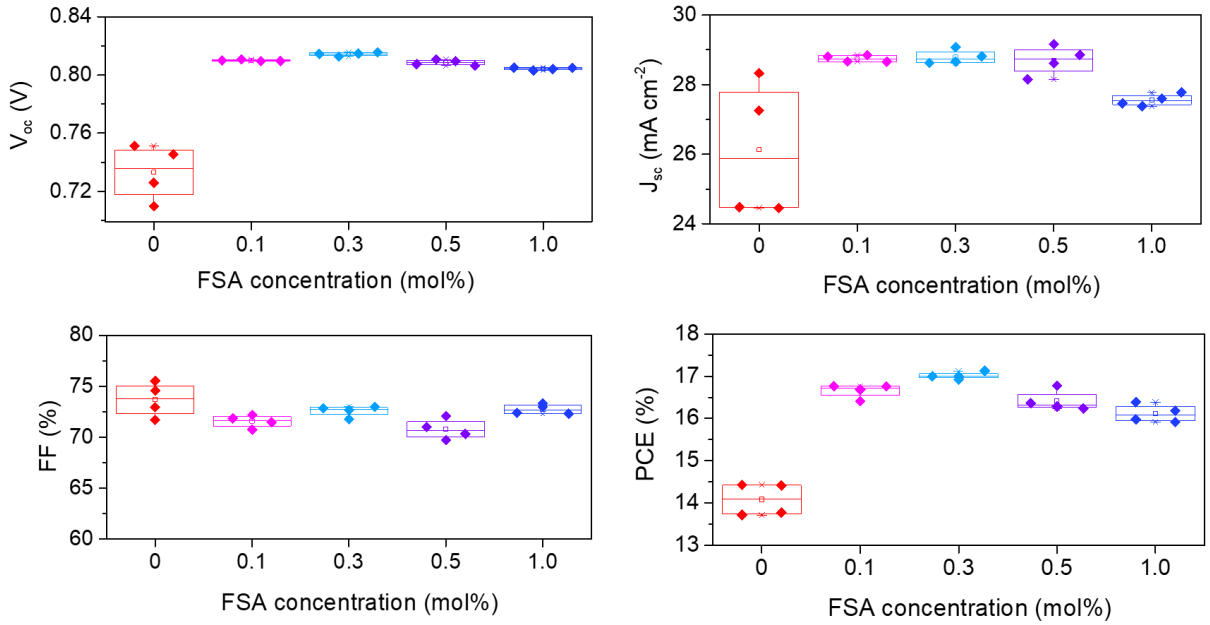

Supplementary Figure 10. Photovoltaic performance of mixed Pb-Sn single-junction solar cells with various FSA concentration. Four devices (with an aperture area of 1.05 cm^2) were processed for each concentration in the same batch. The best performance was achieved at the FSA concentration of 0.3 mol%.

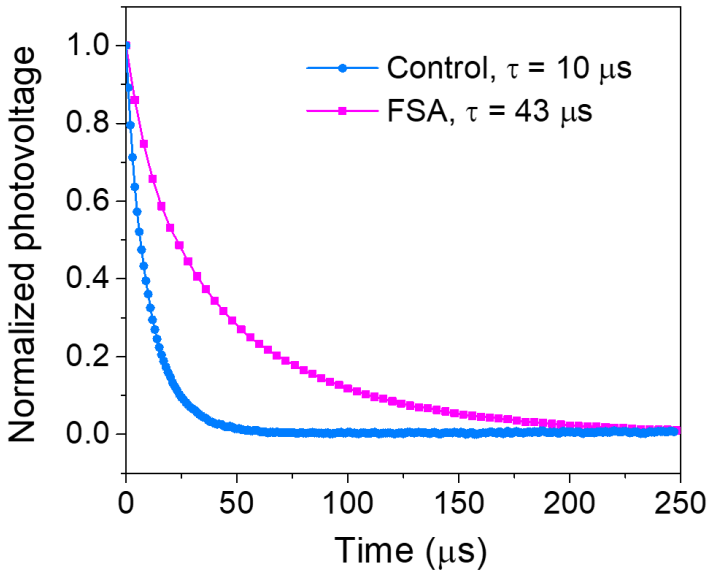

Supplementary Figure 11. Transient photovoltage decays of control and FSA mixed Pb-Sn PSCs. The curves were fitted monoexponentially, showing charge recombination lifetimes of 10 and 43 μs, respectively.

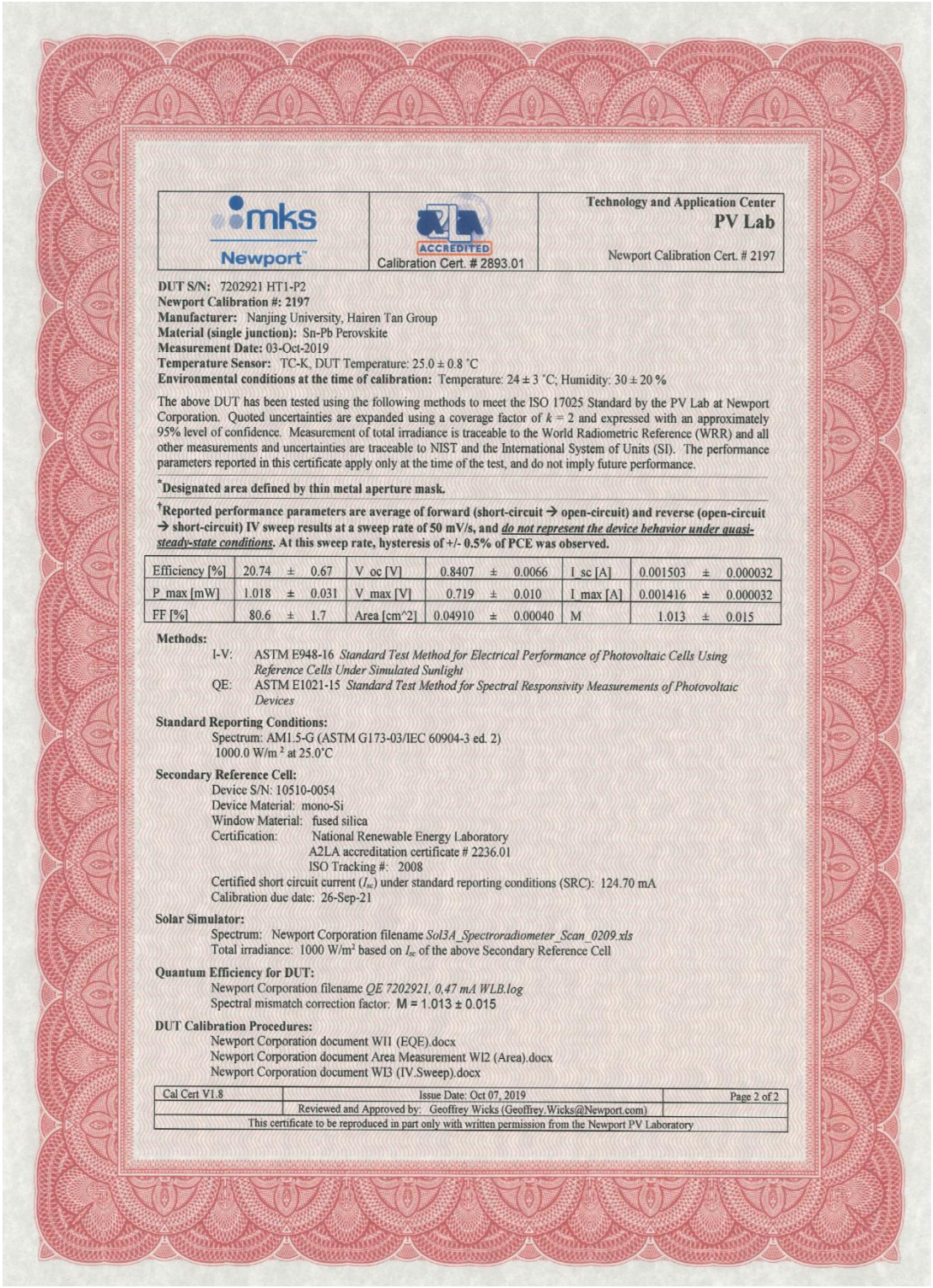

mks Newport

ACCREDITED Calibration Cert. # 2893.01

Technology and Application Center
PV Lab
Newport Calibration Cert. # 2197

DUT S/N: 7202921 HT1-P2
Newport Calibration #: 2197
Manufacturer: Nanjing University, Hairen Tan Group
Material (single junction): Sn-Pb Perovskite
Measurement Date: 03-Oct-2019
Temperature Sensor: TC-K, DUT Temperature: 25.0 ± 0.8 °C
Environmental conditions at the time of calibration: Temperature: 24 ± 3 °C; Humidity: 30 ± 20 %

The above DUT has been tested using the following methods to meet the ISO 17025 Standard by the PV Lab at Newport Corporation. Quoted uncertainties are expanded using a coverage factor of $k = 2$ and expressed with an approximately 95% level of confidence. Measurement of total irradiance is traceable to the World Radiometric Reference (WRR) and all other measurements and uncertainties are traceable to NIST and the International System of Units (SI). The performance parameters reported in this certificate apply only at the time of the test, and do not imply future performance.

***Designated area defined by thin metal aperture mask.**

†Reported performance parameters are average of forward (short-circuit → open-circuit) and reverse (open-circuit → short-circuit) IV sweep results at a sweep rate of 50 mV/s, and *do not represent the device behavior under quasi-steady-state conditions*. At this sweep rate, hysteresis of +/- 0.5% of PCE was observed.

Efficiency [%]	20.74	±	0.67	V_oc [V]	0.8407	±	0.0066	I_sc [A]	0.001503	±	0.000032
P_max [mW]	1.018	±	0.031	V_max [V]	0.719	±	0.010	I_max [A]	0.001416	±	0.000032
FF [%]	80.6	±	1.7	Area [cm^2]	0.04910	±	0.00040	M	1.013	±	0.015

Methods:
I-V: ASTM E948-16 *Standard Test Method for Electrical Performance of Photovoltaic Cells Using Reference Cells Under Simulated Sunlight*
QE: ASTM E1021-15 *Standard Test Method for Spectral Responsivity Measurements of Photovoltaic Devices*

Standard Reporting Conditions:
Spectrum: AM1.5-G (ASTM G173-03/IEC 60904-3 ed. 2)
1000.0 W/m^2 at 25.0°C

Secondary Reference Cell:
Device S/N: 10510-0054
Device Material: mono-Si
Window Material: fused silica
Certification: National Renewable Energy Laboratory
A2LA accreditation certificate # 2236.01
ISO Tracking #: 2008
Certified short circuit current (I_{sc}) under standard reporting conditions (SRC): 124.70 mA
Calibration due date: 26-Sep-21

Solar Simulator:
Spectrum: Newport Corporation filename *Sol3A_Spectroradiometer_Scan_0209.xls*
Total irradiance: 1000 W/m^2 based on I_{sc} of the above Secondary Reference Cell

Quantum Efficiency for DUT:
Newport Corporation filename *QE 7202921, 0,47 mA WLB.log*
Spectral mismatch correction factor: M = 1.013 ± 0.015

DUT Calibration Procedures:
Newport Corporation document WI1 (EQE).docx
Newport Corporation document Area Measurement WI2 (Area).docx
Newport Corporation document WI3 (IV.Sweep).docx

Supplementary Figure 12. **The certified result of mixed Pb-Sn narrow-bandgap perovskite solar cell measured at *Newport*.** The device exhibits a certified PCE of 20.74% with low hysteresis (Forward scan: V_{oc}=0.842 V, J_{sc}=30.59 mA cm^{-2}, FF=80.1%, and PCE=20.63%; Reverse scan: V_{oc}=0.839 V, J_{sc}=30.63 mA cm^{-2}, FF=81.1%, and PCE=20.84%).

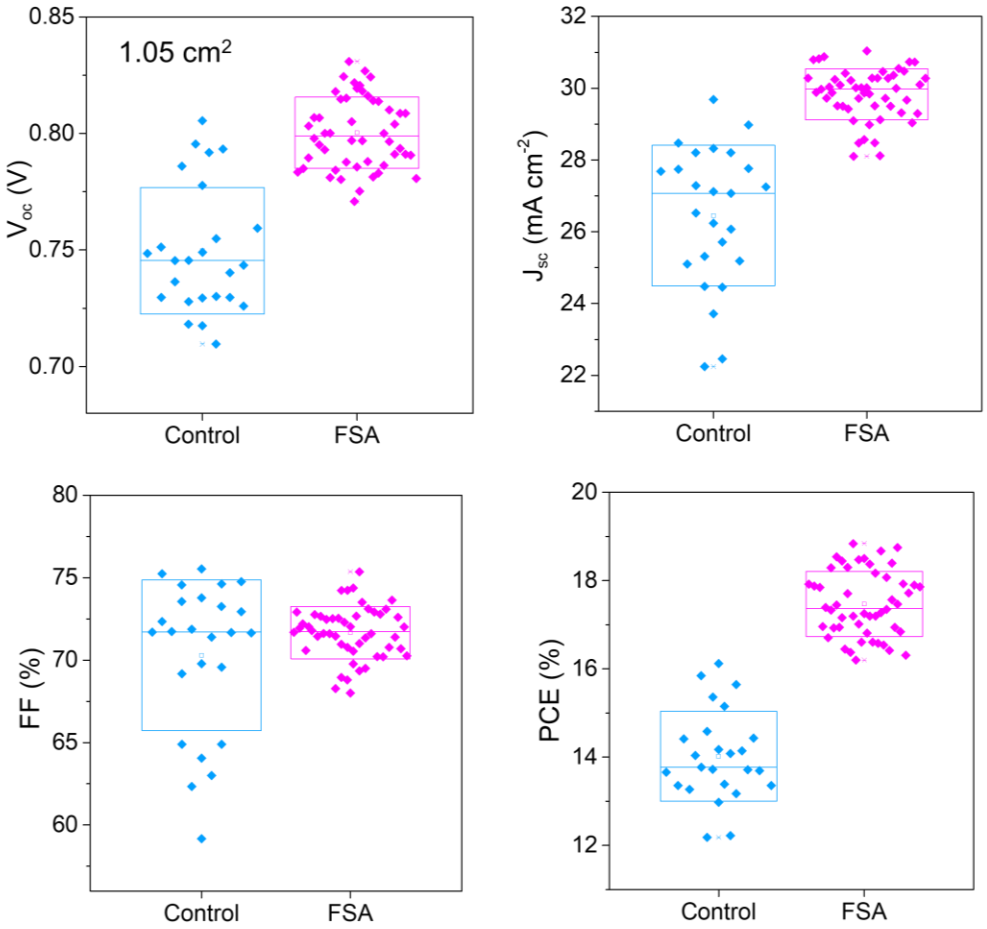

Supplementary Figure 13. Performance comparison of mixed Pb-Sn solar cells. Comparison of photovoltaic performance between 25 control and 50 FSA narrow-bandgap mixed Pb-Sn solar cells (aperture area 1.05 cm^2) processed over several identical runs. The box lines indicate the standard deviation and the center represents the mean value.

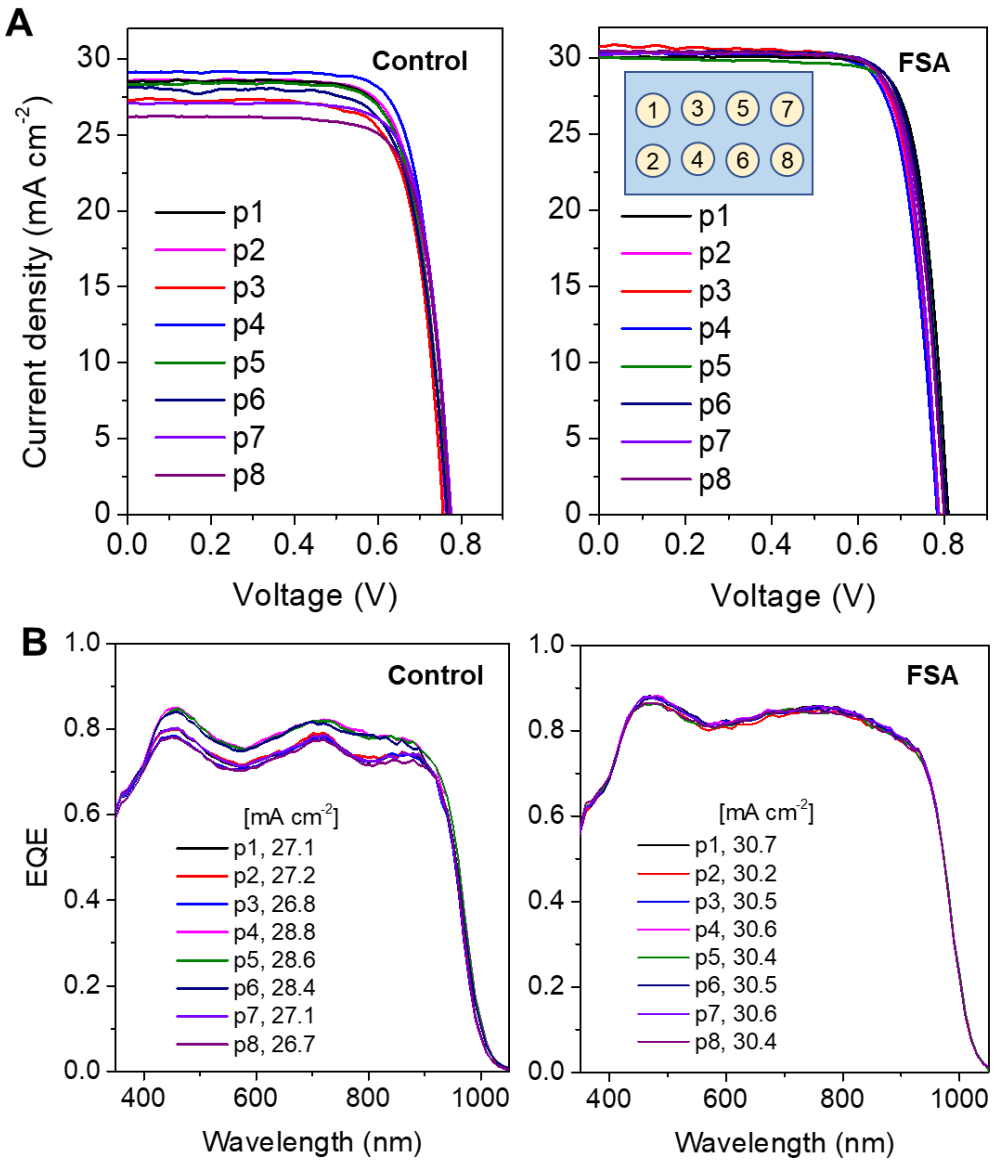

Supplementary Figure 14. Performance distribution of control and FSA Pb-Sn solar cells. (A) J-V curves and **(B)** EQE spectra of control and FSA Pb-Sn solar cells (aperture area of 1.05 cm^2) as measured with a mask having 8 selected small-size (0.049 cm^2) apertures. The J-V and EQE curves were measured with only one aperture open while keeping other aperture closed with a black tape. The inset shows the pixel positions (p1-p8) as defined by small-size apertures over the active area of large-size devices.

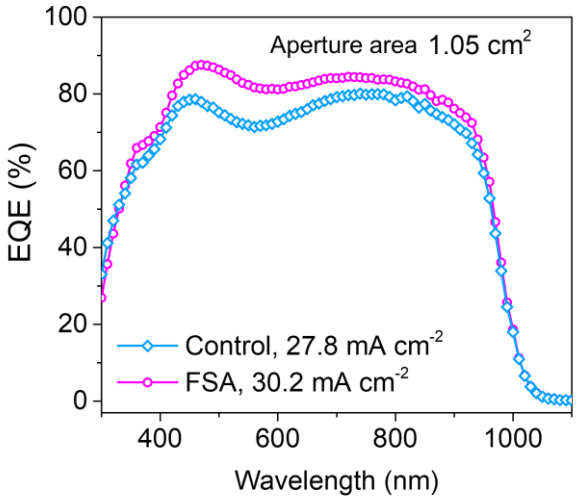

Supplementary Figure 15. EQE spectra of champion control and FSA mixed Pb-Sn solar cells with an aperture area of 1.05 cm^2.

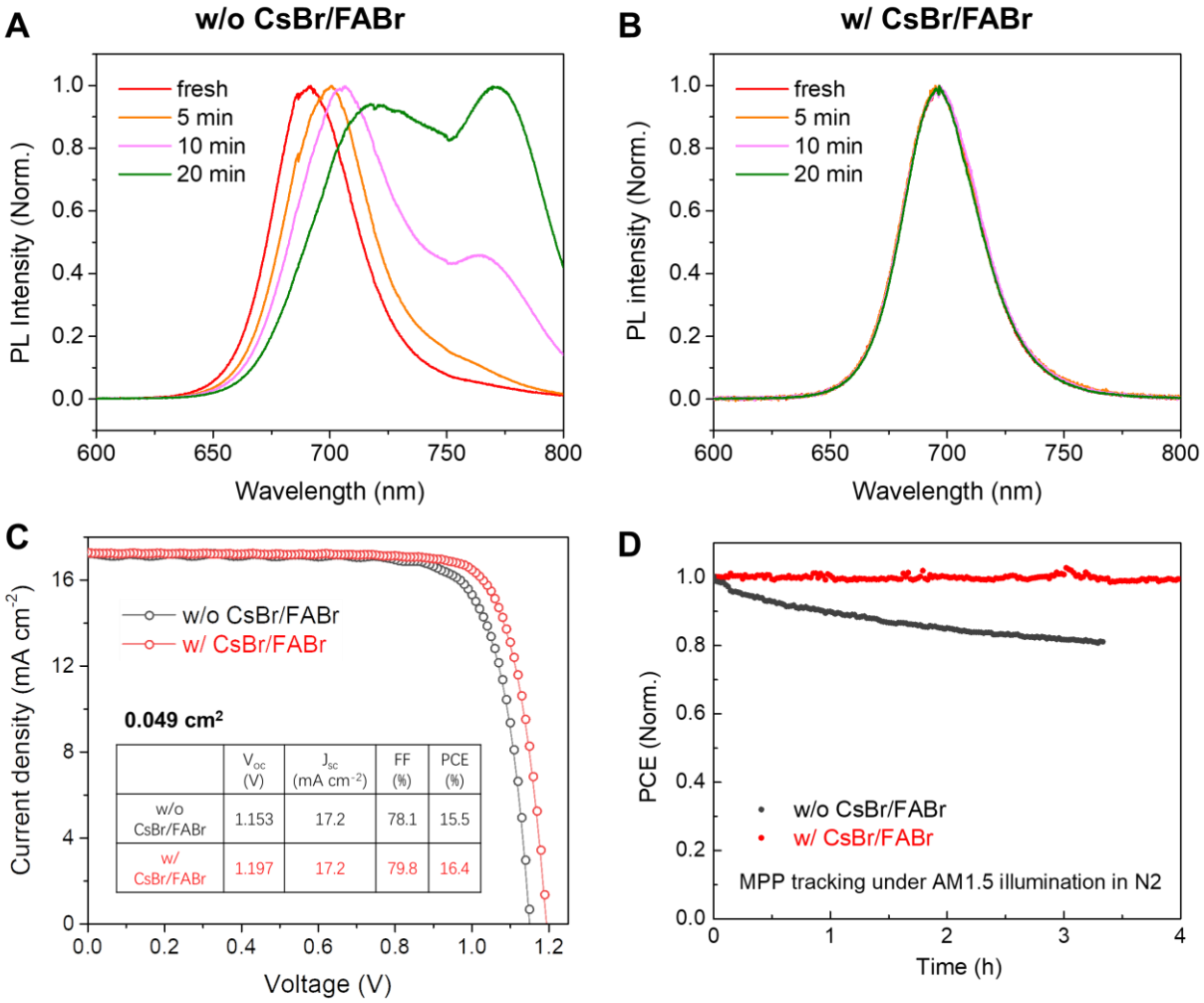

	V_{oc} (V)	J_{sc} (mA cm^{-2})	FF (%)	PCE (%)
w/o CsBr/FABr	1.153	17.2	78.1	15.5
w/ CsBr/FABr	1.197	17.2	79.8	16.4

Supplementary Figure 16. Photostability of wide-bandgap perovskites fabricated from four precursors (CsI, FAI, PbI_2, and $PbBr_2$; denoted w/o CsBr/FABr) or six precursors (CsI, CrBr, FAI, FABr, PbI_2, and $PbBr_2$; denoted w/ CsBr/FABr). (**A,B**) PL spectra of perovskite films after illumination (white LED, intensity equivalent to AM1.5 @100 mW cm^{-2}) for various duration. The film made from four precursors exhibited an obvious photo-induced halide segregation after illumination. (**C**) J-V curves of wide-bandgap perovskite solar cells made from four precursors and six precursors under reverse scans. (**D**) MPP tracking of wide-bandgap perovskite solar cells (shown in **C**) in N_2 glovebox without encapsulation.

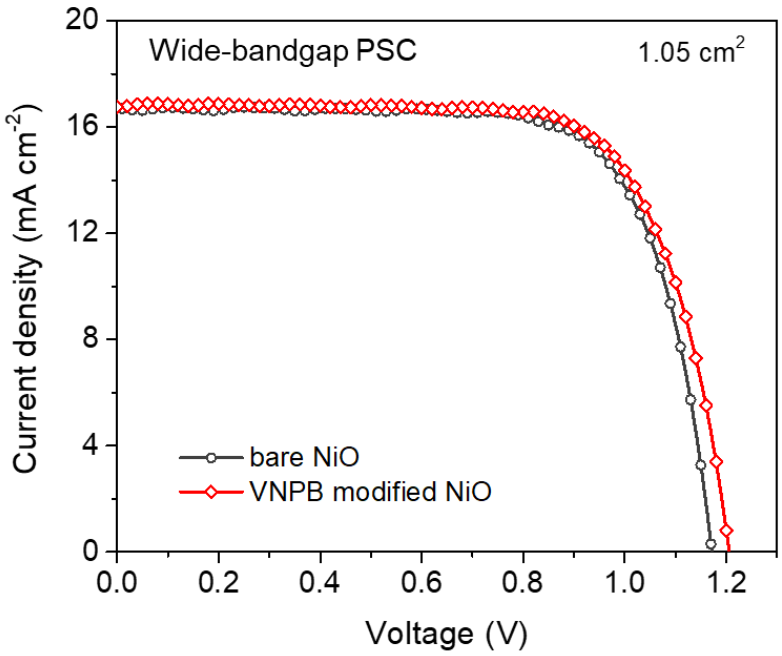

Supplementary Figure 17. J-V curves of wide-bandgap PSCs with bare NiO and VNPB modified NiO as the HTL. The devices were processed in the same run and had an aperture area of 1.05 cm^2.

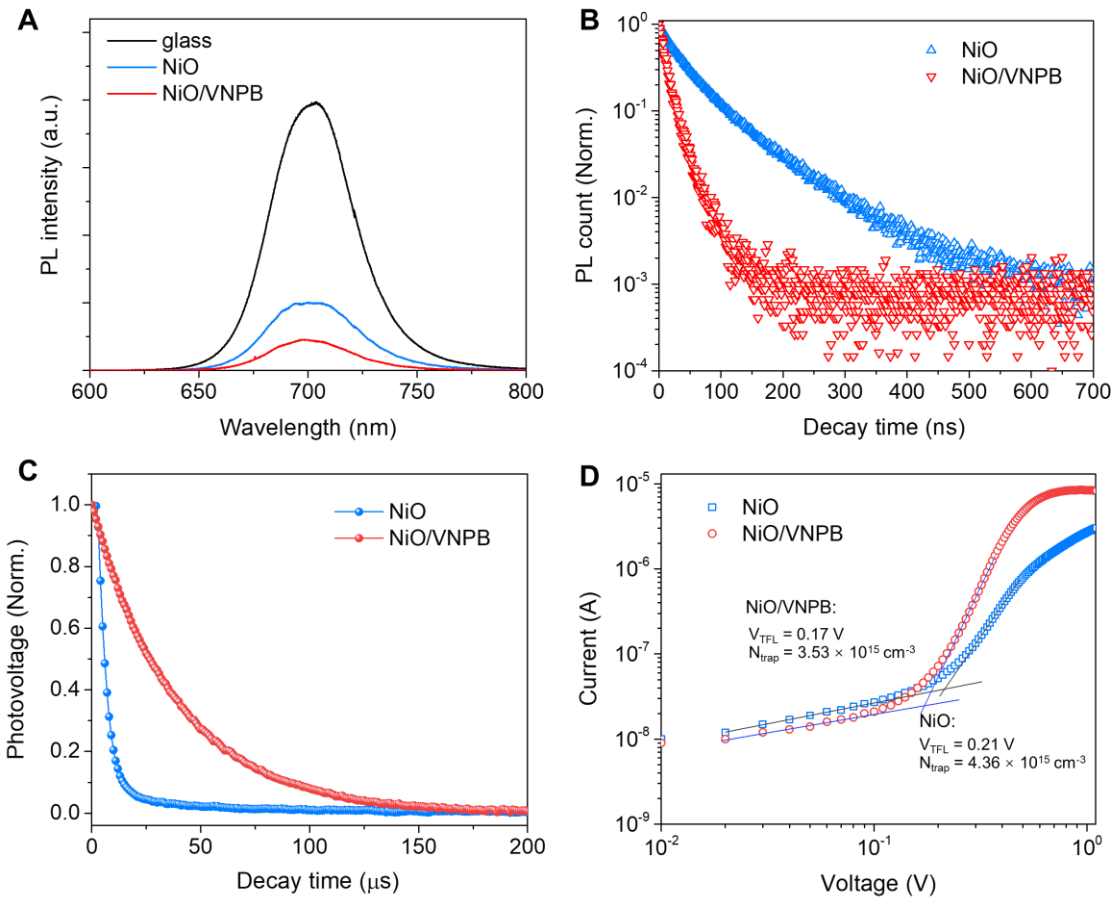

Supplementary Figure 18. Charge dynamics at the interface between NiO and wide-bandgap perovskite. (**A**) Steady-state PL spectra and (**B**) time-resolved PL decay of perovskite films deposited on NiO and NiO/VNPB. (**C**) Transient photovoltage decay of wide-bandgap perovskite solar cells with NiO and NiO/VNPB. The curves were fitted monoexponentially. (**D**) Current-voltage traces and trap density of wide-bandgap perovskites as determined by the SCLC method with the hole-only device structure. The trap density N_{trap} is determined by the equation: $V_{TFL}=qN_{trap}L^2/(2\varepsilon\varepsilon_0)$, where V_{TFL} is trap-filled limit voltage, L the thickness of perovskite film, ε the relative dielectric constant of perovskite, and ε_0 the vacuum permittivity.

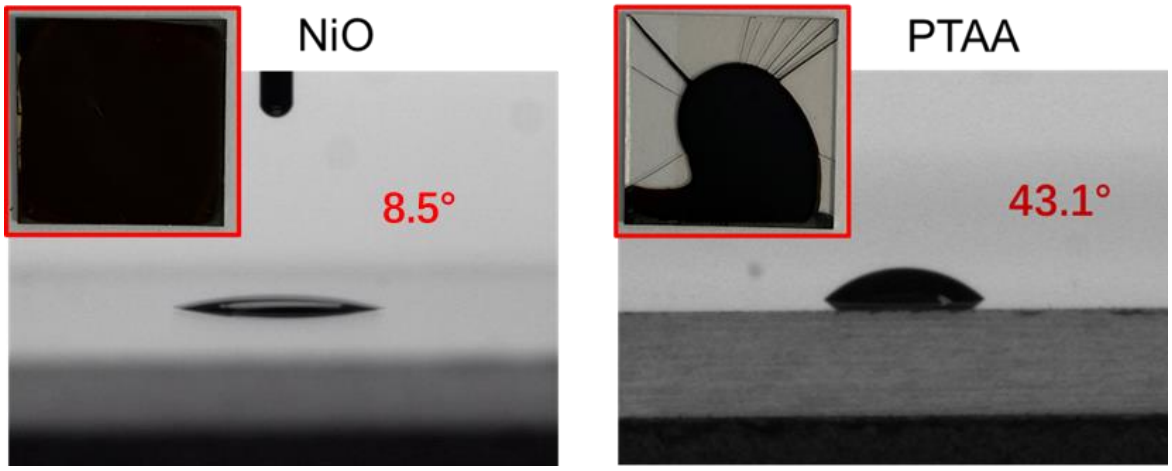

Supplementary Figure 19. Contact angle of perovskite precursor solution on NiO (left) and PTAA (right) films. The precursor solution has excellent wetting property on NiO film, leading to full surface coverage after spin-coating. However, the wetting on PTAA film is poor due to the large contact angle. The film cannot be fully covered by spin-coating without additional spreading of precursor solution on substrates.

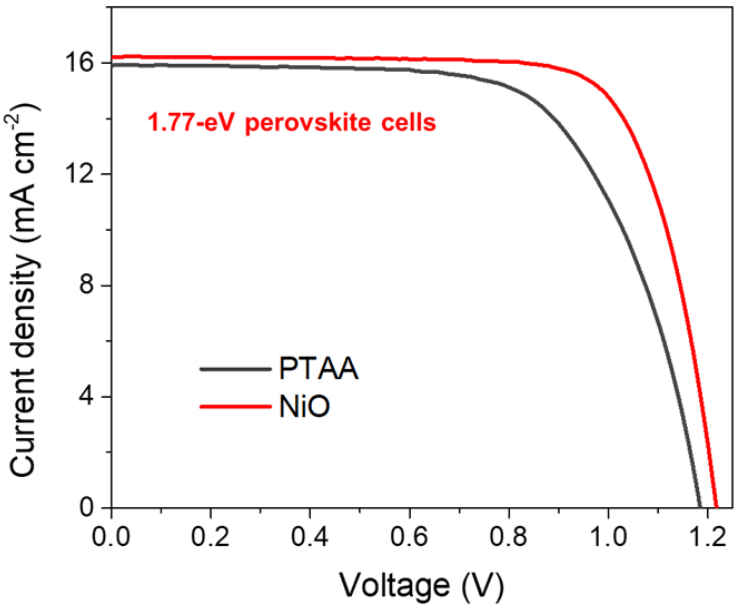

Supplementary Figure 20. Wide-bandgap perovskite solar cell on different HTL. Typical J-V curves of wide-bandgap perovskite solar cells (aperture area 1.05 cm^2) using PTAA and VNPB modified NiO as HTL.

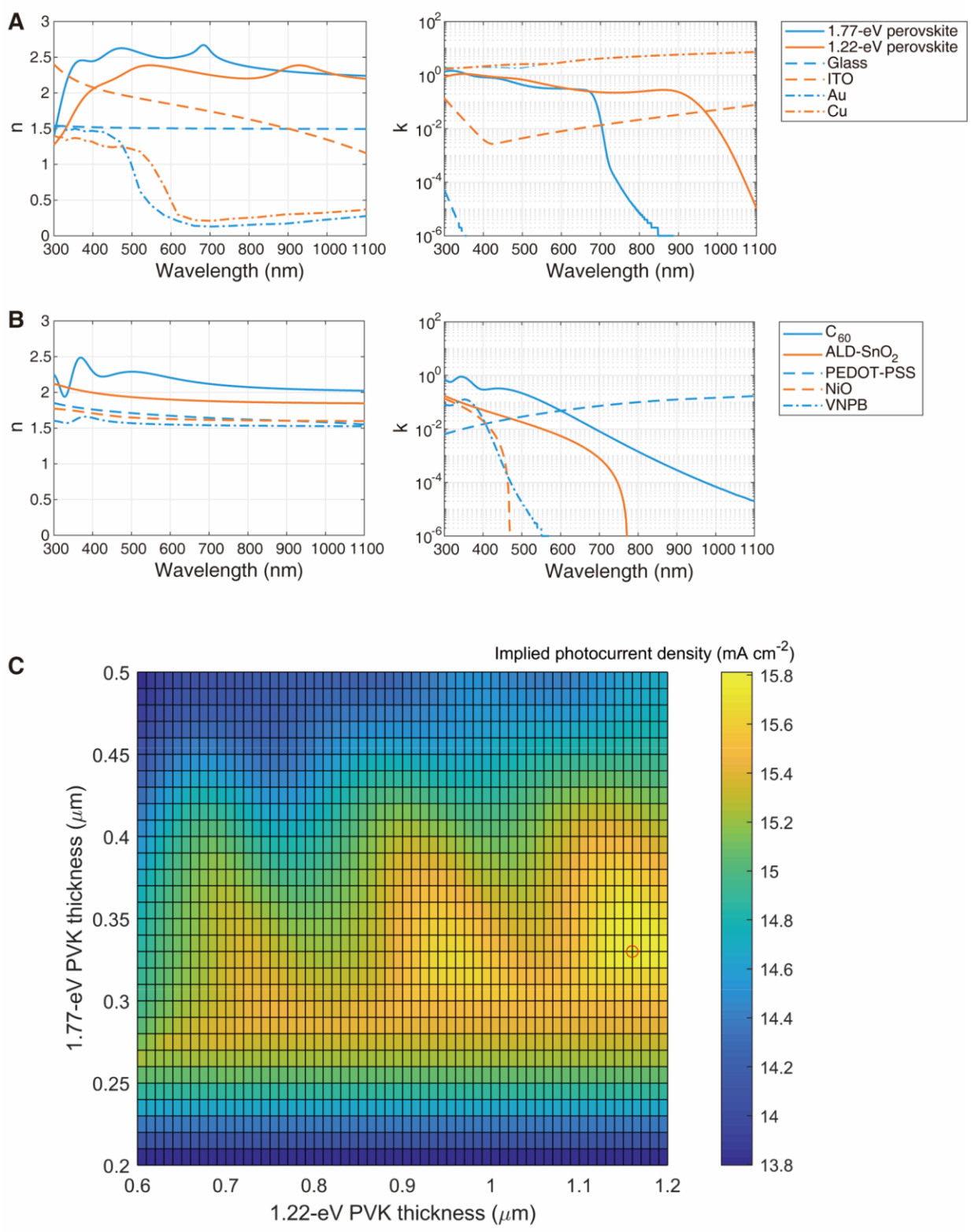

Supplementary Figure 21. Optical simulation of all-perovskite tandem solar cells. (**A-B**) Refractive index (*n*, *k*) of each layer. (**C**) Simulated J_{sc} of all-perovskite tandem solar cells as function of wide-bandgap and narrow-bandgap perovskite layer thicknesses.

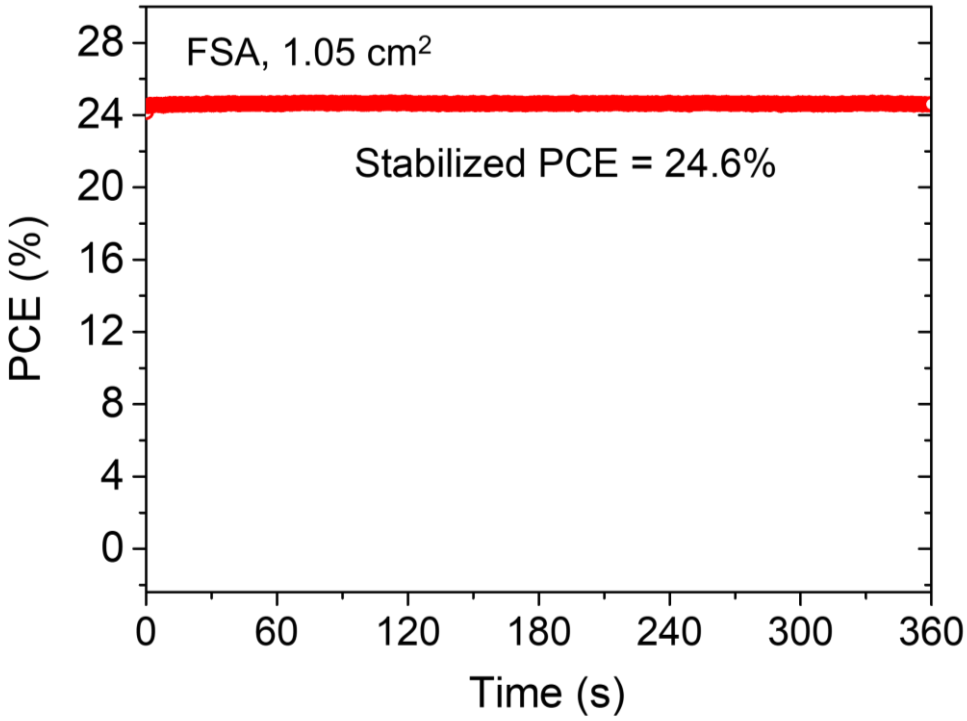

Supplementary Figure 22. Stabilized power output of champion FSA tandem solar cell with an aperture area of 1.05 cm^2.

測定成績書番号(Reference No. 19TR-PV0048)

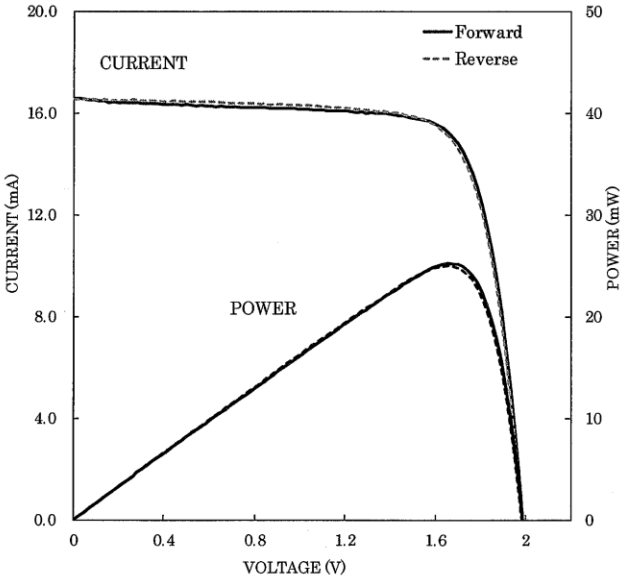

Date : Dec. 21st, 2019
Manufacturer: Hairen Tan Group, Nanjing University
Type: Perovskite/perovskite
2T tandem solar cells
Sample No.: HT-1
Repeat Times. : 1

	Forward	Reverse	
Isc	16.58	16.55	[mA]
Voc	1.986	1.982	[V]
Pmax	25.24	25.02	[mW]
Ipmax	15.24	15.11	[mA]
Vpmax	1.656	1.656	[V]
F.F.	76.63	76.23	[%]
Eff.(Da)	24.2	24.0	[%]
M.Temp	25.1	24.7	[℃]
D Irr.	100.0	100.0	[mW/cm²]
M Irr.(top)	99.9	99.9	[mW/cm²]
M Irr.(bot)	104.1	104.1	[mW/cm²]

Ref. Device No.
JETp-A01W (top) / AK-110 (bot)
Cal. Val. of Ref.
45.12 (top) / 14.96 (bot)
[mA at 100mW/cm²]

JET

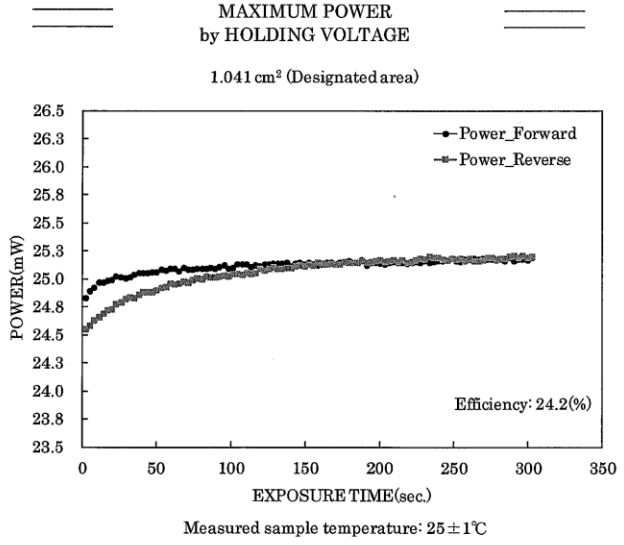

Measured sample temperature: 25±1℃

Date : Dec. 21st, 2019
Manufacturer: Hairen Tan Group
Nanjing University
Type: Perovskite/perovskite
2T tandem solar cells
Sample No.: HT-1

	Forward	Reverse	
Pmax (at 300sec.)	25.19	25.20	[mW]
Ipmax	15.21	15.21	[mA]
Vpmax	1.656	1.656	[V]
Eff.(Da)	24.2	24.2	[%]
D Irr.	100.0	100.0	[mW/cm²]
M Irr.(top)	99.9	99.9	[mW/cm²]
M Irr.(bot)	104.1	104.1	[mW/cm²]

JET

Supplementary Figure 23. The certificated result of 1-cm^2-area monolithic all-perovskite tandem solar cell measured by *JET*. The device shows a stabilized PCE of 24.2% and a PCE of 24.2% under the forward J-V scan (V_{oc}=1.986 V, J_{sc}=15.93 mA cm^{-2}, and FF=76.63%).

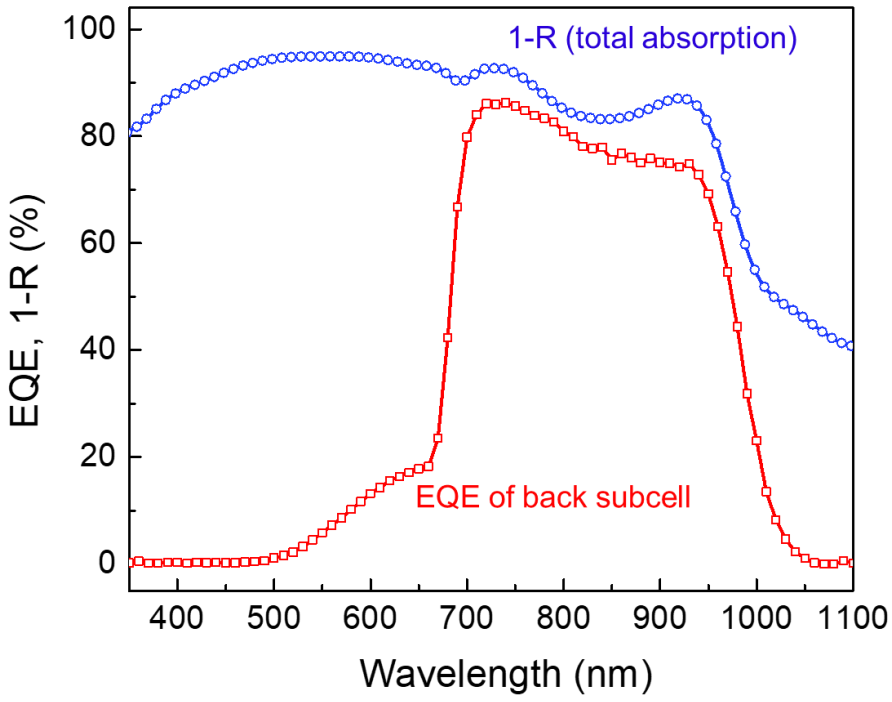

Supplementary Figure 24. The 1-R (total absorption) and EQE (back subcell) spectra of a representative all-perovskite tandem cell. There is a reflection peak at long wavelengths between 750 and 950 nm. R represents the optical reflectance measured from the front side of solar cells.

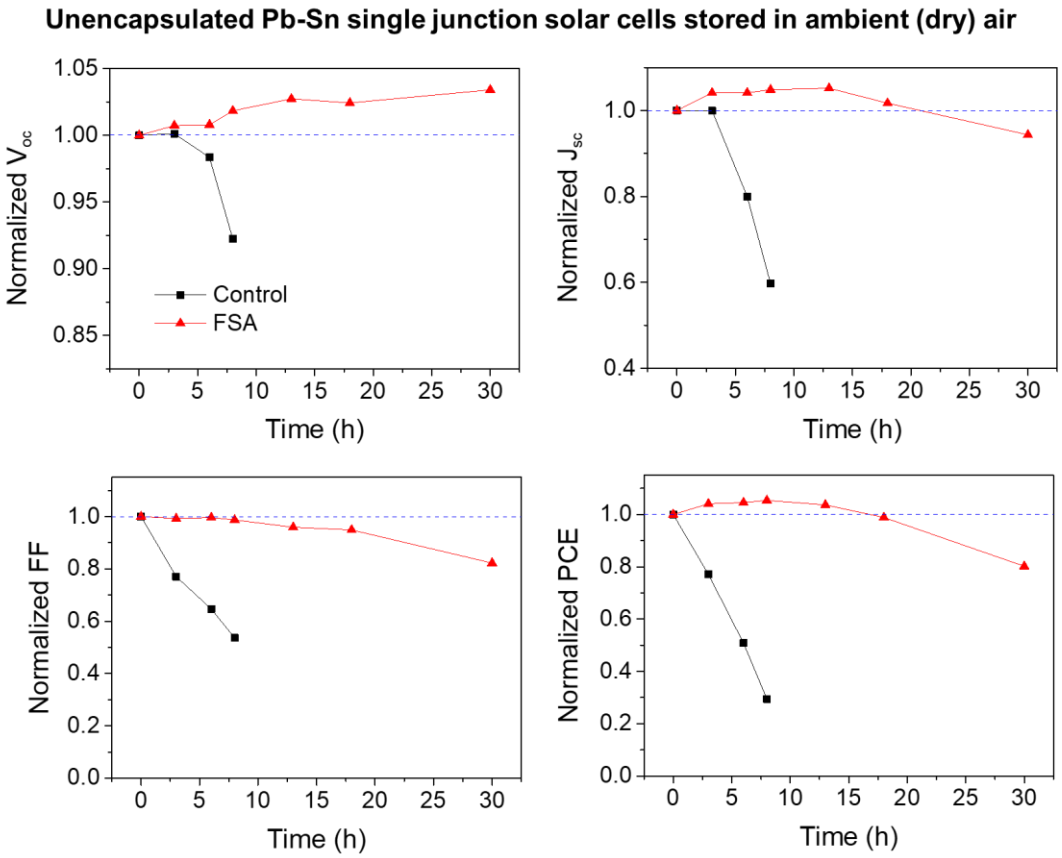

Supplementary Figure 25. Atmospheric stability of Pb-Sn single junction solar cells (aperture area 1.05 cm^2) stored in ambient air with a humidity <20%. The control devices exhibited fast degradation in performance after exposure to air. The FSA samples showed much better tolerance to air exposure and could maintain their initial performance for the first 15 hours. The devices had a structure of glass/ITO/PEDOT:PSS/perovskite/C_{60}/BCP/Cu. The control device had an initial PCE of 15.1%, with a V_{oc} of 0.755 V, a J_{sc} of 27.2 mA cm^{-2}, and a FF of 73.6%; the FSA device had an initial PCE of 18.2%, with a V_{oc} of 0.830 V, a J_{sc} of 30.1 mA cm^{-2}, and a FF of 72.8%.

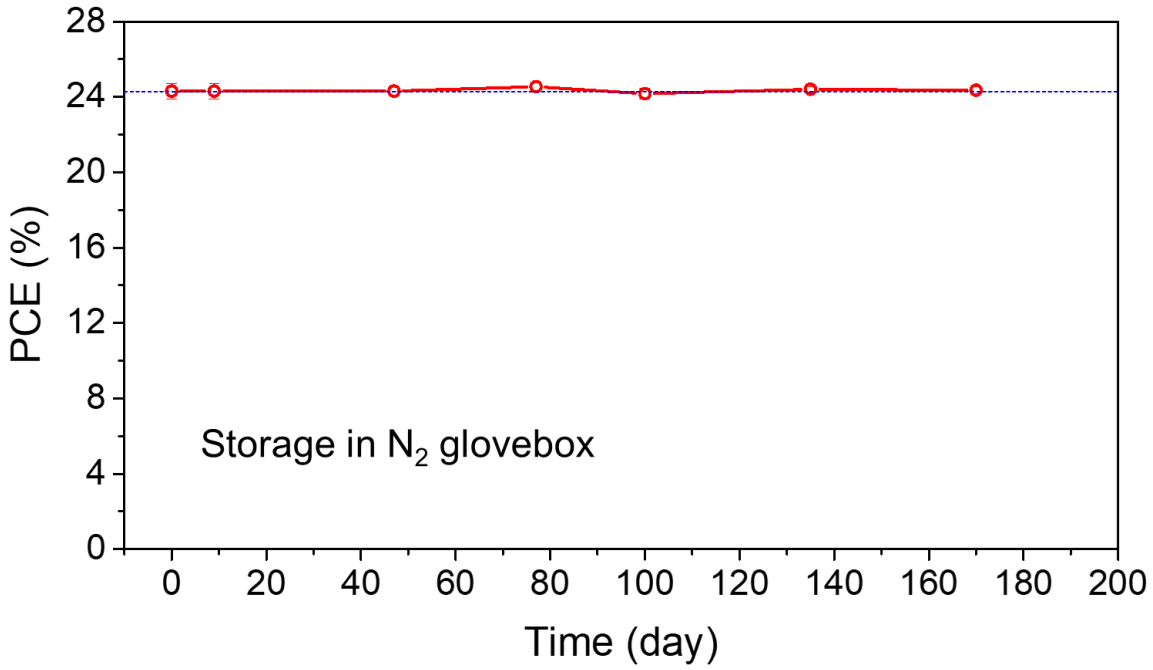

Supplementary Figure 26. Shelf stability of tandem solar cells (aperture area of 1.05 cm^2) under storage in N_2 glovebox. The devices exhibited no obvious degradation in performance after storage for 170 days.

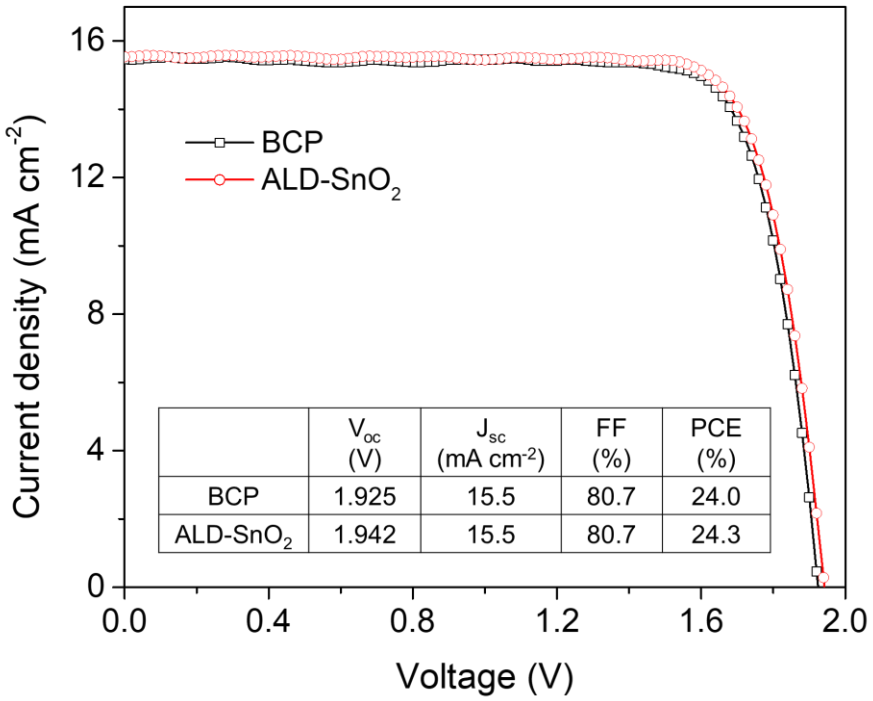

Supplementary Figure 27. Typical J-V curves of FSA all-perovskite tandem solar cells with BCP or ALD-SnO_2 as the ETL for the Pb-Sn subcells. The cells were processed in the same run.

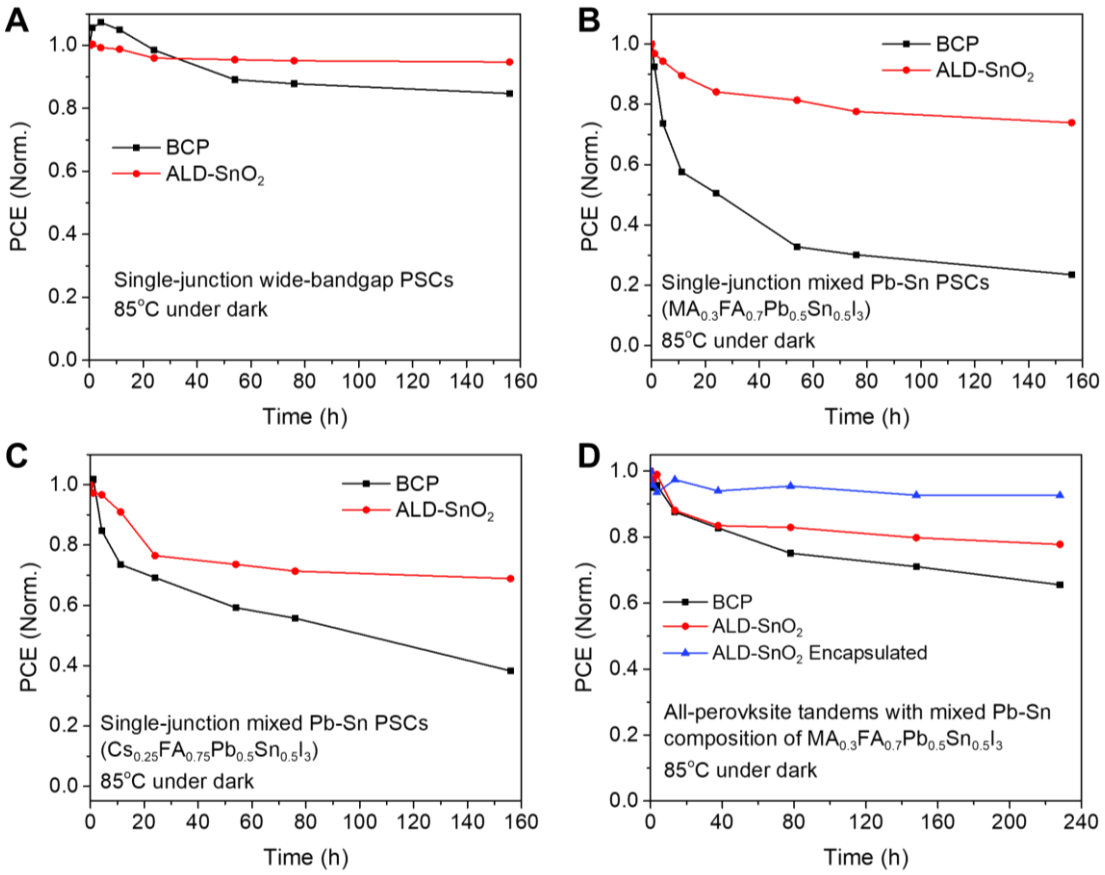

Supplementary Figure 28. Thermal stability of perovskite solar cells at 85ºC under dark. The devices were placed on a hotplate without light illumination in a N_2 glovebox. All mixed Pb-Sn perovskite layers have FSA here. The devices have an aperture area of 0.049 cm^2. (**A**) Single-junction wide-bandgap PSCs with BCP or ALD-SnO_2 as the ETL. (**B**) Single-junction mixed Pb-Sn narrow-bandgap PSCs with BCP or ALD-SnO_2 as the ETL, where the perovskite layers have a composition of $MA_{0.3}FA_{0.7}Pb_{0.5}Sn_{0.5}I_3$. (**C**) Single-junction mixed Pb-Sn narrow-bandgap PSCs with BCP or ALD-SnO_2 as the ETL, where the perovskite layers have a composition of $Cs_{0.25}FA_{0.75}Pb_{0.5}Sn_{0.5}I_3$. (**D**) All-perovskite tandem solar cells with BCP or ALD-SnO_2 as the ETL for the back subcell, where the narrow-bandgap perovskite a composition of $MA_{0.3}FA_{0.7}Pb_{0.5}Sn_{0.5}I_3$. Tandem devices with ALD-SnO_2 as ETL and pressure-tight encapsulation is included as well. Mixed Pb-Sn perovskites were processed with FSA additive. Each data point is an average of four devices for each type. The initial values are provided in Supplementary Table 4.

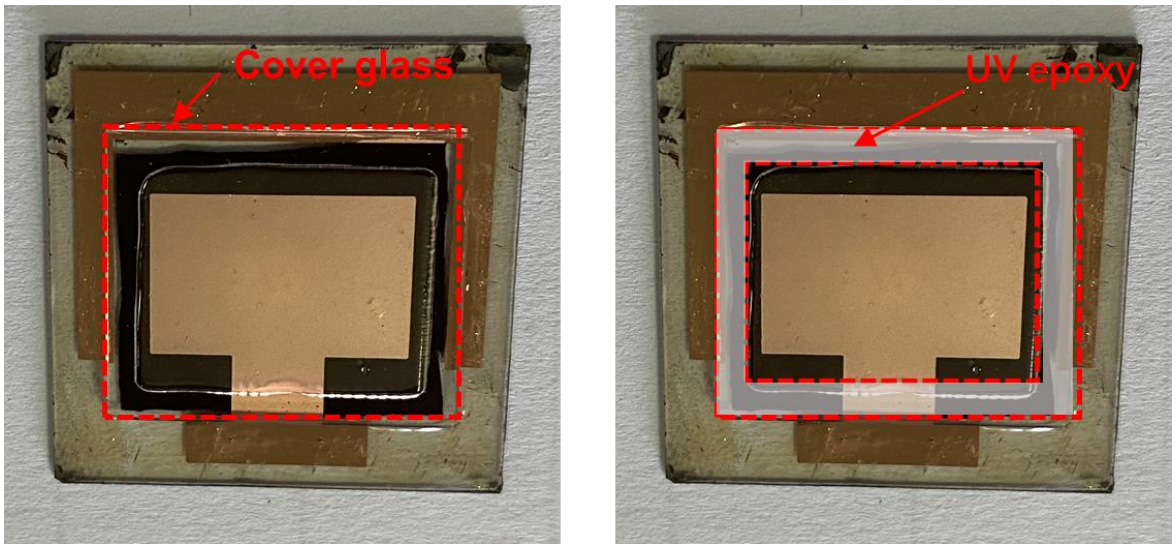

Supplementary Figure 29. Encapsulation of all-perovskite tandem solar cells. The cover glass has a cavity inside to make sure that there is no direct contact between the active area of solar cell and the cover glass. The UV-epoxy is attached around the edges of cover glass and should not contact with the active area of solar cell. It should be noted that perovskite outside the encapsulation area is better to be removed before the encapsulation.

Supplementary Table 1. Photovoltaic parameters of 8 areas measured from the control and FSA Pb-Sn solar cells as shown in Supplementary Fig. 14.

Control

Pixel #	**V_{oc} (V)**	**J_{sc} (mA cm^{-2})**	**FF (%)**	**PCE (%)**
P1	0.764	28.5	75.6	16.5
P2	0.764	28.5	75.6	16.5
P3	0.757	27.3	74.4	15.3
P4	0.774	29.1	76.2	17.2
P5	0.769	28.5	74.0	16.2
P6	0.766	28.3	74.5	16.2
P7	0.775	28.1	73.2	15.8
P8	0.772	27.1	76.1	16.0
Average	0.768	28.2	75.0	16.2

FSA

Pixel #	V_{oc} (V)	J_{sc} (mA cm^{-2})	FF (%)	PCE (%)
P1	0.810	30.0	79.3	19.3
P2	0.787	30.4	77.8	18.6
P3	0.788	30.8	77.2	18.7
P4	0.784	30.4	77.0	18.4
P5	0.804	30.0	78.1	18.9
P6	0.803	30.4	78.6	19.2
P7	0.786	30.2	79.1	18.8
P8	0.800	30.5	77.5	18.9
Average	0.795	30.3	78.1	18.8

Supplementary Table 2. Independently certified best efficiencies of thin-film solar cells with areas over 1 cm^2.

	Cell type	**Area** (cm^2)	**V_{oc}** (V)	**J_{sc}** (mA cm^{-2})	**FF** (%)	**PCE** (%)	**Group**	**Ref.**
Single junction	CIGS	1.043	0.734	39.58	80.4	23.4	Solar Frontier	[1]
	CdTe	1.062	0.876	30.25	79.4	21.0	First Solar	[1]
	PVK	1.024	1.193	21.64	83.6	21.6	ANU	[1]
	OPV	1.023	0.842	23.28	68.6	13.5	Uni Potsdam	[1]
	DSSC	1.005	0.744	22.47	71.2	11.9	Sharp	[1]
	CZTSSe	1.176	0.533	33.57	63.0	11.3	DGIST, Korea	[1]
	a-Si:H	1.044	0.550	29.72	75.0	11.9	AIST	[1]
2T-tandem	a-Si/nc-Si	1.000	1.342	13.45	70.2	12.7	AIST	[1]
	PVK/CIGS	1.035	1.683	19.17	72.1	23.3	HZB	[1]
	PVK/PVK	**1.041**	**1.986**	**15.93**	**76.6**	**24.2**	**Nanjing Uni**	**This work**

CIGS: copper indium gallium selenide; PVK: perovskite; OPV: organic solar cell; DSSC: dye-sensitized solar cell

Supplementary Table 3. Initial PV parameters of the devices shown in Figure 5a. Each data point is an average of four devices for each type.

Device	**V_{oc} (V)**	**J_{sc} (mA cm^{-2})**	**FF (%)**	**PCE (%)**
Control_BCP	1.885	14.3	81.1	21.9
FSA_BCP	1.929	15.2	80.5	23.7
Control_ALD-SnO_2	1.927	14.1	81.1	22.0
FSA_ALD-SnO_2	1.941	15.2	81.0	23.9

Supplementary Table 4. Initial PV parameters of the devices shown in Supplementary Figure 28. Each data point is an average of four devices for each type. Note that the devices shown in Supplementary Figure 28 were processed during the revision of the manuscript. We found that the mixed Pb-Sn perovskite solar cells exhibited lower performance than the devices shown in Figure 3.

Panel #	**Device**	**V_{oc} (V)**	**J_{sc} (mA cm^{-2})**	**FF (%)**	**PCE (%)**
A	BCP	1.178	16.9	75.3	15.0
	ALD-SnO_2	1.174	16.7	77.4	15.1
B	BCP	0.816	30.8	78.9	19.8
	ALD-SnO_2	0.778	30.5	79.2	18.8
C	BCP	0.727	29.9	75.7	16.5
	ALD-SnO_2	0.717	29.8	75.0	16.1
D	BCP	1.925	15.5	80.2	23.9
	ALD-SnO_2	1.932	15.2	80.6	23.7
	ALD-SnO_2 encapsulated	1.895	15.6	79.5	23.5

Supplementary Table 5. Processing parameters of ALD-SnO_2 layer used for all-perovskite tandem solar cells.

	Chamber Temp. (℃)	TDMASn Source Temp. (℃)	TDMASn pulse time (s)	Purge time (s)	Water pulse time (s)	Purge time (s)	Cycle
Interconnecting layer	100	60	0.05	6	0.02	6	250
ETL for Pb-Sn subcell	70	60	0.04	7	0.02	5	150

Supplementary Table 6. Fitting parameters used for Fig. 2b. The PL decay curves were fitted with biexponential components to obtain a fast and a slow decay lifetime (τ_1 and τ_2). The mean carrier lifetimes (τ) for the biexponential fit were calculated by the weighted average method: $\tau = (A_1\tau_1 + A_2\tau_2)/(A_1+A_2)$.

Sample	**A_1**	**τ_1 (ns)**	**A_2**	**τ_2 (ns)**	**Effective lifetime (ns)**
FSA	1.4253	79.9	0.3478	631.0	188
Control	0.6825	29.0	0.3468	134.0	64

References:

[1] Green, M. A. *et al.* Solar cell efficiency tables (Version 55). *Prog. Photovoltaics Res. Appl.* **28**, 3–15 (2020).